Huete, César; Sánchez, Antonio L. Williams, Forman A. (2017). Diffusion-Flame Ignition by Shock-Wave Impingement on a Hydrogen-Air Supersonic Mixing Layer. *Journal of Propulsion and Power*, 33(1), 256-263.

DOI: https://doi.org/10.2514/1.B36236

Diffusion-Flame Ignition by Shock-Wave Impingement on a Hydrogen-Air Supersonic Mixing Layer

César Huete*
Universidad Carlos III, 28911 Leganés, Spain
Antonio L. Sánchez† and Forman A. Williams‡
University of California San Diego, La Jolla, CA 92093-0411

Ignition in a supersonic hydrogen-air mixing layer interacting with an oblique shock wave is investigated analytically under conditions such that the post-shock flow is supersonic and the peak post-shock temperature prior to ignition remains below the crossover temperature. The study requires consideration of the flow structure in the post-shock ignition kernel found around the point of maximum temperature, which is assumed in this study to lie at an intermediate location across the mixing layer, as occurs in mixing layers subject to significant viscous dissipation. The ignition kernel displays a balance between the rates of chemical reaction and post-shock flow expansion, including the acoustic interactions of the chemical heat release with the shock wave leading to increased front curvature. The problem is formulated with account taken of the strong temperature dependence of the chemical heat-release rate characterizing the ignition chemistry in the low-temperature regime analyzed here. It is shown how consideration of a two-step reduced chemical-kinetic mechanism derived in previous work leads to a boundary-value problem that can be solved analytically to determine ignition as a fold bifurcation, with the turning point in the diagram of peak perturbation induced by the chemical reaction as a function of the Damköhler number providing the critical conditions for ignition.

Nomenclature

D	Ignition Damköhler number defined in (22)
$I^{\pm}$	Characteristic variables defined in (7)
$J^{\pm}$	Rescaled characteristic variables
M	Mach number
n	Local transverse coordinate pointing towards the air side
p, $\hat{p}$	Pressure, nondimensional pressure variation
T, $\hat{T}$	Temperature, nondimensional temperature variation
T_c	Crossover temperature
s	Local streamwise distance along the post-shock streamline that departs from $z = z_o$
V, $\hat{V}$	Transverse velocity, nondimensional transverse velocity
β	Nondimensional activation energy
δ	Characteristic mixing-layer thickness defined in (1)
Δ	Normalized Damköhler number defined in (34)
ϕ	Downstream-flow inclination with respect to the shock
φ	Rescaled H_2O_2 concentration defined in (30)
κ	Mixing-layer parameter defined in (29)
$\bar{\lambda}, \lambda$	Heat-release parameters defined in (23) and (34)

*Assistant Professor, Grupo de Mecánica de Fluidos, Universidad Carlos III de Madrid.
†Professor, Department of Mechanical and Aerospace Engineering, University of California San Diego.
‡Professor, Department of Mechanical and Aerospace Engineering, University of California San Diego. AIAA Fellow.

Λ Nondimensional pressure loss per unit length along the streamlines
μ Angle of inclination of the two Mach lines with respect to the local flow direction
ν Clockwise flow deflection across the shock
ρ Density
σ Incident angle
θ Temperature perturbation induced by the chemical reaction

Subscript

F Frozen flow
o Flow properties at $z = 0$

Superscript

$'$ Properties upstream from the shock

I. Introduction

Mixing layers and shock waves are two different phenomena that coexist in hypersonic and supersonic propulsion devices. For instance, in supersonic-combustion ramjets (SCRAMJETS), shock waves are typically generated ahead of the combustion zone, where the supersonic incoming flow enters a converging nozzle and interacts with wedged walls and fuel injectors. Along its path through the combustor, the flow is subject to complex shock trains and expansion waves.[1]

In SCRAMJETS, shock waves can interact with the flow in many different ways. For instance, shocks may disturb the flow near the walls leading to sudden transition to turbulence and augmented wall heating in boundary layers. The corresponding shock/boundary-layer interaction problem is one of high practical relevance that has received a large amount of attention in recent years.[2,3] A relatively less known interaction occurs when shocks impinge on chemically reacting mixing layers of fuel and oxidizer. To illustrate the relevance of shock/mixing-layer interaction phenomena, consider the following standard fuel-injection configurations employed in SCRAMJETS. In one configuration, the shock waves interact with the mixing layer that separates the supersonic incoming hot-air stream and the subsonic fuel flow, and which is generated downstream from a strut fuel injector (see Figs. 5 and 11 in Ref.[4]). Similarly, in configurations with jet-in-crossflow fuel injection, a reflected bow shock interacts with the mixing layer generated from the aerodynamics of the fuel jet as it flows into the supersonic incoming hot-air stream (see, for instance, Fig. 4 in Ref.[5]). In all cases, since the residence time of the reactants in the combustor is short in supersonic regimes, ignition typically cannot be achieved by relying on diffusion and heat conduction alone.[6] Shock waves may help, however, to heat the mixture and speed-up the mixing process,[7–10] the former arising from the inherent temperature rise across the shock wave, and the latter associated with the interaction of the shock with the non-uniform flow.[11]

Although the aerodynamic interactions described above are predominantly encountered in highly turbulent flows in practical applications, analytical solutions to related simplified laminar problems can be advantageous in studying such supersonic-combustion processes, helping to clarify the real configuration, not only for increasing understanding but also for suggesting scaling concepts that may prove useful in formulating subgrid-scale models. A simplified laminar configuration involving a supersonic mixing layer subjected to impingement by a shock from the air stream was considered in our recent ignition study,[12] which adopted a model one-step irreversible reaction with large activation energy to describe the chemical heat release. The present paper employes the same laminar-flow configuration to investigate low-temperature ignition in hydrogen-air systems, with the model chemistry of the previous work replaced by a two-step reduced mechanism that provides a sufficiently accurate description of the underlying ignition chemistry under the conditions investigated here.[13]

Autoignition processes in hydrogen-air systems depend in a fundamental way on the existing temperature, with two distinguished regimes emerging from the competition of radical recombination by the elementary reaction $H + O_2 + M \rightarrow HO_2 + M$ with the chain-branching path controlled by $H + O_2 \rightarrow OH + O$. Equating the rates of radical production and radical consumption defines the so-called crossover temperature T_c, whose value depends on the pressure through the presence of the third-body concentration in the resulting equation, giving $T_c \simeq 950$ K and $T_c \simeq 1500$ K for $p = 1$ atm and $p = 100$ atm, respectively. Fast radical branching leading to a branched-chain explosion occurs only for temperatures above this crossover value, such that the rate of H-atom production becomes larger than that of termination. If the post-shock conditions place

the system above crossover, then ignition is expected to occur following a rapid chain-branching explosion with little influence from the post-shock expansion associated with the shock curvature. For weaker shocks such that the post-shock temperature remains below crossover, ignition occurs instead as a slow thermal explosion, which is very sensitive to the small temperature variations resulting from the flow expansion behind the curved shock. Determination of the critical conditions in this low-temperature ignition regime requires detailed consideration of acoustic-thermal interactions in the ignition kernel,[12] as done below on the basis of reduced chemistry.

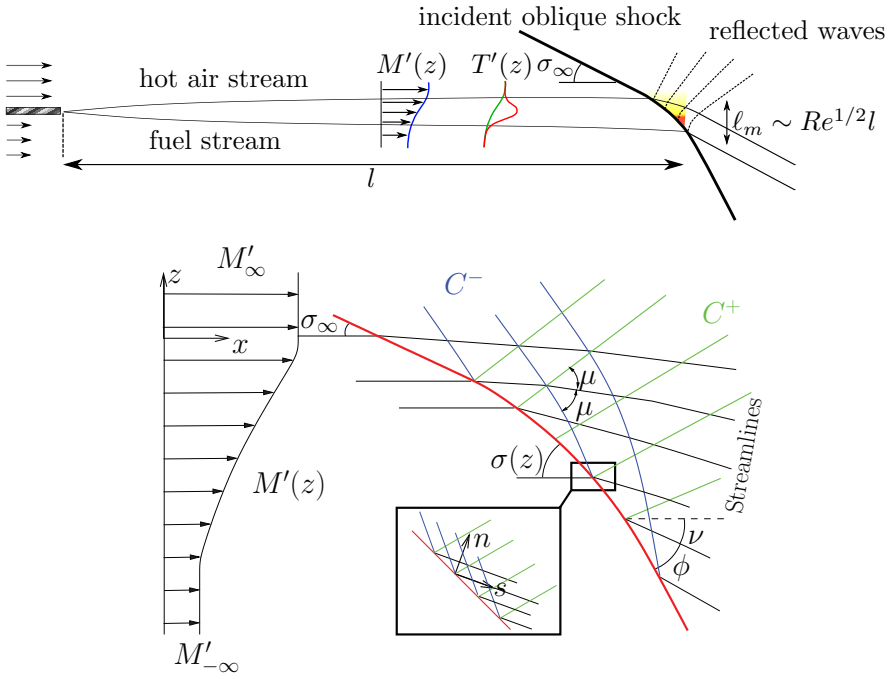

Figure 1. Sketch of the model problem.

II. Model problem

The specific model configuration investigated here considers a laminar mixing layer separating supersonic parallel streams of air and hydrogen moving at different velocities. An oblique shock wave generated on the air side with initial incident angle σ_∞ impinges on the mixing layer at a given downstream location, as shown in the schematic view of Fig. 1, where the air stream is located on the upper side. The interaction of the shock with the mixing layer results in a complicated free-boundary problem in which the shape of the curved shock front, defined by the incident angle σ, is coupled to the post-shock flow.[14] The solution requires integration of the Euler equations downstream from the shock. At the shock, the different properties can be evaluated in terms of σ and the local Mach number M' for a given value of the specific-heat ratio γ by use of the Rankine-Hugoniot relations. The solution simplifies when the post-shock flow remains supersonic, that being the case considered in the present analysis. The Euler equations can be formulated in characteristic form, with three different characteristic lines crossing any given point, i.e., the streamline and the two Mach lines C^+ and C^-, as indicated in Fig. 1, with different characteristic equations applying along each of them.

For the ignition analysis, it is of interest that, under most conditions, the C^+ characteristic lines issuing from the shock represent an expansion wave that reduces the pressure (and therefore the temperature) along the streamlines, so that the peak temperature is found immediately downstream from the shock. Then, because of the strong temperature sensitivity of the chemical reaction, we find in the vicinity of the shock front a small ignition kernel where the incipient chemical reaction is competing with the flow expansion. Critical conditions for ignition can be determined, following the approach proposed by Frank-Kamneteskii when analyzing thermal explosions in closed vessels, by examining whether weakly reactive solutions exist in this ignition kernel. If heat-release rates are too large, then such solutions fail to exist, corresponding

to ignition having occurred. A novel aspect is that, for these shock-induced ignition problems, the cooling processes that compete with the chemical heat release involve inviscid gas dynamic acoustic-wave propagation instead of the familiar diffusive heat conduction.

A relevant feature of supersonic mixing layers is the fact that, while the Mach number distribution across the mixing layer $M'(z)$ typically decreases monotonically with the distance from the air boundary, when the existing shear is sufficiently high and the temperature difference between the two streams is not too pronounced the shape of the transverse temperature profile may develop a maximum at an intermediate location as a result of the effect of viscous dissipation. Because of the strong temperature dependence of the chemical reaction rate, the ignition kernel is always located around the high-temperature region, resulting in two different ignition scenarios depending on whether the transverse temperature profile displays a peak at the air boundary or at an intermediate location inside the mixing layer, as was recognized by the early researchers analyzing spontaneous thermal ignition in high-speed mixing layers.[15,16] Similarly, two different regimes emerge in connection with shock-induced ignition events, as discussed in a recent study[12] employing one-step Arrhenius heat release chemistry with a large activation energy. Both regimes lead to fold-bifurcation descriptions of ignition in a Frank-Kamenetskii approach.

The present paper extends our recent contribution[12] by incorporating heat-release chemistry for hydrogen-air mixing layers. Attention is restricted to ignition events occurring in the interior of the mixing layer, corresponding to configurations in which the temperature of the chemically frozen solution immediately behind the shock exhibits a peak value $T = T_o$ at an intermediate location $z = z_o$. Furthermore, the conditions considered pertain to fairly weak shocks, leading to peak post-shock temperatures below the so-called crossover temperature, under which conditions ignition occurs as a thermal explosion rather than a branched-chain explosion, the latter being characteristic of high-temperature hydrogen-air ignition.[13] At these low-temperature conditions, all chemical intermediates accurately follow a steady-state approximation in the ignition regime, thereby justifying a two-step chemical-kinetic reduced mechanism, which has been shown to provide excellent accuracy in descriptions of low-temperature ignition events, including homogeneous ignition times,[17] mixing-layer ignition distances in shock-free configurations,[18] and critical explosion conditions in closed vessels.[19] It will be shown below that use of this reduced chemistry reduces the shock-induced ignition problem to a boundary-value problem that can be solved analytically.

III. Formulation

Since the chemical reaction displays a strong temperature dependence, ignition occurs near the point $z = z_o$ where the post-shock temperature of the chemically frozen solution reaches its peak value. The local weakly reactive flow can be described as a perturbation to the frozen solution using a cartesian coordinate system that includes the streamwise distance s along the post-shock streamline that departs from $z = z_o$ and the associated transverse coordinate n pointing towards the air side. As in our previous work,[12] both coordinates are scaled with the characteristic mixing-layer thickness

$$\delta = \frac{\sin\phi_o}{\sin\sigma_o}\left(\frac{\mathrm{d}M'}{\mathrm{d}z}\right)^{-1}_{z=z_o}, \tag{1}$$

which is defined for definiteness from the gradient of Mach number distribution $\mathrm{d}M'/\mathrm{d}z$, with σ_o and ϕ_o being the local values of the incident angle and of the downstream-flow inclination with respect to the shock. A sketch indicating the local coordinate system is given in the inset of Fig. 1, the relevant angles also being indicated on the figure.

III.A. Linearized Euler equations

The governing equations for the flow are obtained by linearizing the reactive Euler equations around the post-shock solution found at $z = z_o$, where the temperature, pressure, density, Mach number, and streamwise velocity take the values T_o, p_o, ρ_o, M_o, and $U_o = M_o\sqrt{(\gamma-1)c_pT_o}$, with c_p denoting the specific heat at constant pressure. The procedure is identical to that used in classical textbooks[20] when deriving characteristic equations for supersonic isentropic flows, with the condition of constancy of entropy replaced in our analysis by the equations describing the chemical heat release along the streamlines. We begin by writing the conservation equations in their primitive form and proceed to derive the characteristic equations, including

characteristic variables $I^{\pm}$ that effectively replace the pressure and transverse velocity in the integration along the Mach lines C^+ and C^-.

The problem can be formulated in terms of the pressure and temperature perturbations $\hat{p} = (p - p_o)/p_o$ and $\hat{T} = (T - T_o)/T_o$ and the ratio $\hat{V} = V/U_o$ of the transverse velocity V to the unperturbed velocity U_o. These dimensionless variables can be used to write the streamwise and transverse components of the momentum balance equation in the form

$$\frac{\gamma M_o^2 - 1}{\gamma M_o^2}\frac{\partial \hat{p}}{\partial s} - \frac{\partial \hat{T}}{\partial s} + \frac{\partial \hat{V}}{\partial n} = 0 \tag{2}$$

$$\gamma M_o^2 \frac{\partial \hat{V}}{\partial s} + \frac{\partial \hat{p}}{\partial n} = 0, \tag{3}$$

after the continuity equation and the equation of state are used to express the perturbations of density and streamwise velocity in terms of $\hat{p}$, $\hat{T}$, and $\hat{V}$. In terms of these variables, the energy and species conservation equations for a reactive mixture with N different chemical species become

$$\frac{\partial \hat{T}}{\partial s} - \frac{\gamma - 1}{\gamma}\frac{\partial \hat{p}}{\partial s} = -\sum_{i=1}^{N}\left(\frac{h_i^o}{\rho_o c_p T_o}\right)\left(\frac{\dot{C}_i}{U_o/\delta}\right) \tag{4}$$

and

$$\frac{\partial C_i}{\partial s} = \frac{\dot{C}_i}{U_o/\delta}, \tag{5}$$

where C_i, $\dot{C}_i$, and h_i^o denote, respectively, the concentration (mols per unit volume), rate of production by chemical reaction (mols per unit volume per unit time), and molar enthalpy of formation of species i.

The problem can be conveniently formulated in characteristic form by combining linearly (2)–(4) to give

$$\frac{\partial I^{\pm}}{\partial s} \pm \frac{1}{\sqrt{M_o^2 - 1}}\frac{\partial I^{\pm}}{\partial n} = -\frac{\gamma M_o^2}{M_o^2 - 1}\sum_{i=1}^{N}\left(\frac{h_i^o}{\rho_o c_p T_o}\right)\left(\frac{\dot{C}_i}{U_o/\delta}\right) \tag{6}$$

for the characteristic variables

$$I^{\pm} = \hat{p} \pm \frac{\gamma M_o^2}{\sqrt{M_o^2 - 1}}\hat{V}, \tag{7}$$

which can be used to rewrite (4) as

$$\frac{\partial \hat{T}}{\partial s} - \frac{\gamma - 1}{2\gamma}\frac{\partial}{\partial s}(I^+ + I^-) = -\sum_{i=1}^{N}\left(\frac{h_i^o}{\rho_o c_p T_o}\right)\left(\frac{\dot{C}_i}{U_o/\delta}\right). \tag{8}$$

Equations (5), (6), and (8) supplemented with appropriate expressions for the chemical rates $\dot{m}_i$ are the basis for the local description of thermal ignition events in two-dimensional, steady supersonic flows.

As can be inferred from (4) and (5), the species concentrations C_i and the dimensionless entropy perturbation $\hat{T} - (\gamma - 1)\hat{p}/\gamma$ evolve along the streamlines $n =$ constant, while the characteristic variables $I^{\pm}$ are seen in (6) to evolve along the Mach lines

$$C^{\pm}: \quad s + \frac{n}{\tan\phi_o} = \left(\frac{1}{\tan\phi_o} \pm \frac{1}{\tan\mu_o}\right)(n - n_s), \tag{9}$$

involving the local downstream-flow inclination $\phi_o = \sigma_o - \nu_o$ with respect to the shock and the angle of inclination

$$\mu_o = \sin^{-1}\left(\frac{1}{M_o}\right) \tag{10}$$

of the two Mach lines with respect to the local flow direction, with $s + n/\tan\phi_o$ representing the distance from the shock measured along a streamline $n = constant$. Here, n_s denotes the value of n corresponding to the point where the Mach line intersects the shock, whose location is defined in this linear approximation by the straight line $s + n/\tan\phi_o = 0$.

Since the normal component of the velocity behind the shock is subsonic (i.e., $\mu_o > \phi_o$), the C^- characteristics always reach the shock, while the C^+ characteristics originate there. Therefore, in writing the boundary conditions for (5), (6), and (8) we need to specify the values of C_i, $\hat{T}$, and I^+ at the shock, while the boundary value of I^- along a given C^- characteristic must be specified outside the ignition kernel, where we find a linear distribution $I^- \propto n_s$, with the proportionality coefficient determined in general from the numerical computation of the chemically frozen flow for $z > z_o$. The composition does not change across the chemically inert shock, so that the boundary condition along the shock line $s + n/\tan\phi_o = 0$ for the species concentration can be directly evaluated in terms of the transverse distributions $Y_i(z)$ of mass fraction found upstream from the shock according to $C_i = \rho_o Y_i/W_i$, where W_i is the molecular mass of species i. The boundary values of $\hat{T}$ and I^+ can be obtained by analyzing the local jumps of temperature, pressure, and velocity across the shock with use made of the linearized the Rankine-Hugoniot relations, as shown elsewhere.[12]

III.B. The chemistry description

As indicated in the introduction, the present work addresses ignition occurring at post-shock temperatures below the crossover temperature, which is shown in Fig. 2 as a function of the post-shock pressure, for clearer orientation. The heavy line in the figure pertains to stoichiometric hydrogen-air mixtures, there being a dependence on the equivalence ratio because the third-body chaperon efficiency is 2.5 times larger for hydrogen than for oxygen and nitrogen, leading to larger values in fuel-rich mixtures; the shading about the curve spans the full range of possible values. As has been explained,[13] in ignition events below crossover the radicals H, O, and OH are kept at low concentrations by the rapid reactions $H + O_2 + M \rightarrow HO_2 + M$, $H_2 + O \rightarrow OH + H$, and $H_2 + OH \rightarrow H_2O + H$. Correspondingly, under those conditions, the ignition chemistry is dominated by reactions involving HO_2 and H_2O_2, with ignition occurring as a thermal explosion. After an initial stage of HO_2 buildup, its consumption rate by $2HO_2 \rightarrow H_2O_2 + O_2$ becomes dominant, keeping this species also in steady state, with a local concentration that corresponds to the instantaneous production-consumption balance.

To describe the interplay between HO_2 and H_2O_2 leading to the thermal explosion at temperatures below crossover, three rate-controlling elementary reactions need to be considered, namely $H_2O_2 + M \xrightarrow{1} 2OH + M$, $2HO_2 \xrightarrow{2} H_2O_2 + O_2$, and $HO_2 + H_2 \xrightarrow{3} H_2O_2 + H$, whereas initiation reactions such as $H_2 + O_2 \rightarrow HO_2 + H$, which are important in the early stages of time-dependent ignition processes,[17] can be entirely neglected for determining critical explosion conditions. Additional consideration of the rapid removal of OH and H radicals through $OH + H_2 \rightarrow H_2O + H$ and $H + O_2 + M \rightarrow HO_2 + M$ along with introduction of a steady-state assumption for HO_2, motivated by its relatively rapid consumption through $2HO_2 \xrightarrow{2} H_2O_2 + O_2$, readily leads to a simple two-step reduced description involving the overall reactions

$$2H_2 + O_2 \rightarrow 2H_2O, \qquad \text{(I)}$$

and

$$H_2 + O_2 \rightarrow H_2O_2 \qquad \text{(II)}$$

with rates given by

$$\omega_{\rm I} = \omega_1 = k_1 C_{\rm M_1} C_{\rm H_2O_2}. \qquad (11)$$

and

$$\omega_{\rm II} = \omega_3 = k_3 (k_1/k_2)^{1/2} C_{\rm M_1}^{1/2} C_{\rm H_2} C_{\rm H_2O_2}^{1/2}, \qquad (12)$$

with $C_{\rm M_1}$ representing the effective third-body concentration for reaction 1. Expressions for $C_{\rm M_1}$ and for the temperature variation of the constants $k_1(T)$, $k_2(T)$, and $k_3(T)$ can be found in Ref.[13]

The two overall steps I and II, together with their associated rates given in (11) and (12) provide the chemistry description needed to study ignition below crossover. Both steps have distinct necessary roles in the explosion development. Thus, because the heat of reaction associated with I is about four times larger than that of II, the enthalpy released in the formation of H_2O being about twice that of H_2O_2, heat release relies predominantly on the first global step, whereas the second step contributes to the ignition process by creating in an autocatalytic fashion the H_2O_2 needed to enable both reactions to proceed, as dictated by (11) and (12).

The temperature sensitivities of the elementary reactions $H_2O_2 + M \xrightarrow{1} 2OH + M$ and $HO_2 + H_2 \xrightarrow{3} H_2O_2 + H$ are very large, with resulting activation temperatures for the overall reactions I and II, associated

with the coefficients k_1 and $k_3(k_1/k_2)^{1/2}$, that can be seen to be almost identical.[17] Consequently, differences between the two overall activation temperatures can be neglected in the Frank-Kamenetskii linearization of the rates about the peak temperature T_o, which uses the same nondimensional activation temperature β according to

$$\omega_{\rm I} = k_1(T_o) C_{\rm M_1} C_{\rm H_2O_2} e^{\beta\hat{T}} \quad \text{and} \quad \omega_{\rm II} = k_3(T_o)[k_1(T_o)/k_2(T_o)]^{1/2} C_{\rm M_1}^{1/2} C_{\rm H_2} C_{\rm H_2O_2}^{1/2} e^{\beta\hat{T}}. \tag{13}$$

For evaluation purposes one may employ the value $\beta = 24534/T_o - 2.3$ associated with the low-pressure limit of the reaction-rate coefficient k_1,[19] with T_o expressed in Kelvin. For the ignition analysis variations of $C_{\rm H_2}$ and $C_{\rm M_1}$ resulting from the chemical reaction can be neglected in the first approximation in computing the reaction rates (13).

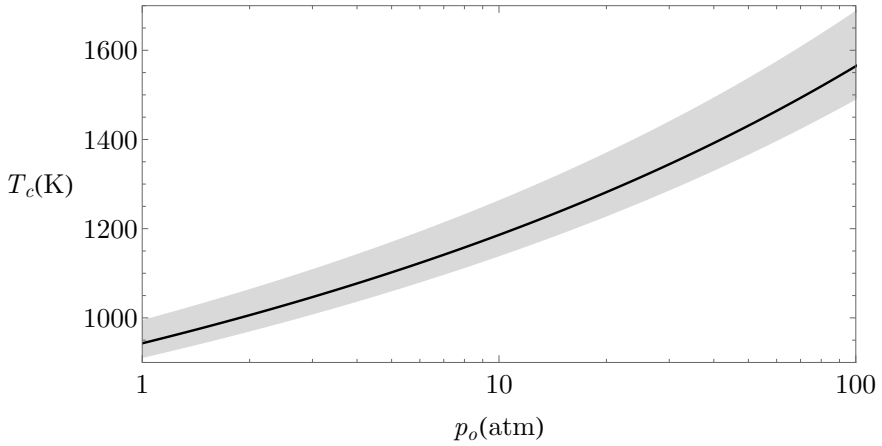

Figure 2. Crossover temperature T_c as a function of the post-shock pressure p_o.

III.C. The ignition kernel

As shown in Ref.,[12] the characteristic size of the ignition kernel can be identified from the temperature distribution found behind the shock when the flow is chemically frozen, given by

$$\hat{T}_F = -\Gamma_T n^2 - \frac{\gamma - 1}{\gamma} \Lambda \left(s + \frac{n}{\tan\phi_o} \right), \tag{14}$$

where $\Lambda = -\partial\hat{p}_F/\partial s$ is the constant value of the normalized pressure loss per unit length along the streamlines, with $s + n/\tan\phi_o$ denoting the distance from the shock measured along a streamline $n =$ constant. Correspondingly, $-\Gamma_T n^2$ measures the post-shock temperature drop from the peak value along the shock, with Γ_T being an order-unity constant. According to (14), the ignition kernel, where the temperature departs from its peak value by an amount of order $\hat{T} \sim \beta^{-1}$, extends over streamwise distances of order $s + n/\tan\phi_o \sim \beta^{-1}$ and much larger transverse distances of order $n \sim \beta^{-1/2}$, suggesting the introduction of the stretched coordinates

$$\xi = \frac{\gamma - 1}{\gamma} \Lambda\beta \left(s + \frac{n}{\tan\phi_o} \right) \quad \text{and} \quad \eta = \Gamma_T^{1/2} \beta^{1/2} n \tag{15}$$

for the description of the ignition kernel.

It is clear from (13) that $\theta = \beta(\hat{T} - \hat{T}_F)$ is the appropriate rescaled temperature variable for describing the small perturbations resulting from the chemical reaction in the ignition regime, yielding

$$e^{\beta\hat{T}} = e^{-\eta^2 - \xi} e^{\theta} \tag{16}$$

for the Frank-Kamenetskii exponential factor carrying the temperature dependence of the chemical reactions (13). The same scaling applies to the departures of the characteristic variables $I^{\pm}$ from their chemically frozen distributions $I_F^{\pm}$, so that we define $J^{\pm} = \beta(I^{\pm} - I_F^{\pm})$. On the other hand, using the simple

order-of-magnitude balances

$$\frac{\partial C_{H_2O_2}}{\partial s} \sim \frac{\omega_{II}}{U_o/\delta} \quad \text{and} \quad \frac{\partial \hat{T}}{\partial s} \sim \left(\frac{-2h^o_{H_2O}}{\rho_o c_p T_o}\right)\left(\frac{\omega_I}{U_o/\delta}\right) \tag{17}$$

stemming from (5) and (8) provides from (13) the expression

$$\frac{C_c}{C_{H_2}} = (\beta q)^{-2/3}\left(\frac{k_3}{(k_1k_2)^{1/2}}\right)^{2/3}\left(\frac{C_{H_2}}{C_{M_1}}\right)^{1/3} \tag{18}$$

for the characteristic value C_c of the H_2O_2 concentration associated with nondimensional temperature increments of order β^{-1}, where $q = (-2h^o_{H_2O}C_{H_2}/(\rho_o c_p T_o)$. The associated rescaled concentration $Y = C_{H_2O_2}/C_c$ is to be employed below for analyzing the ignition problem.

The above scaling (15) indicates that in the limit $\beta \gg 1$ the ignition kernel is thin in the streamwise direction. As a result, when written in terms of the rescaled coordinates ξ and η the conservation equations for $J^{\pm}$ along the Mach lines display a small factor $\beta^{-1/2}$ multiplying the transverse derivatives $\partial J^{\pm}/\partial\eta$. These transverse derivatives can therefore be neglected in the first approximation when the limit $\beta \gg 1$ is considered, reducing the problem to one involving ordinary differential equations rather than partial differential equations, as done in[12] for one-step model chemistry. The same simplification will be adopted now when writing (6) in the ignition kernel for the two-step reduced chemistry defined above.

Rewriting (5), (6), and (8) in terms of the rescaled variables θ, $J^{\pm}$, and Y and the rescaled coordinates ξ and η leads to

$$\frac{\partial Y}{\partial \xi} = DY^{1/2}e^{-\eta^2-\xi}e^{\theta} \tag{19}$$

$$\frac{\partial \theta}{\partial \xi} - \frac{\gamma-1}{2\gamma}\frac{\partial}{\partial \xi}(J^+ + J^-) = D(Y + \bar{\lambda}Y^{1/2})e^{-\eta^2-\xi}e^{\theta} \tag{20}$$

$$\left(1 \pm \frac{\tan\mu_o}{\tan\phi_o}\right)\frac{\partial J^{\pm}}{\partial \xi} = \gamma(\tan^2\mu_o + 1)D(Y + \bar{\lambda}Y^{1/2})e^{-\eta^2-\xi}e^{\theta}, \tag{21}$$

when the approximation of negligible transverse derivatives is incorporated in (21). Here

$$D = \frac{\gamma\beta q}{(\gamma-1)\Lambda}\frac{k_1 C_{M_1} C_c}{C_{H_2}U_o/\delta} \tag{22}$$

is the relevant Damköhler number while the parameter

$$\bar{\lambda} = \frac{h^o_{H_2O_2}}{2h^o_{H_2O}}\left(\frac{k_3^2}{k_1k_2}\right)^{1/2}\left(\frac{C_{H_2}/C_{M_1}}{C_c/C_{H_2}}\right)^{1/2}, \tag{23}$$

typically small, measures the fraction of the heat released by H_2O_2 formation. Outside the ignition kernel the reactive perturbations to the characteristic variable I^- are identically zero, thereby yielding the boundary condition

$$J^- = 0 \quad \text{as} \quad \xi \to \infty. \tag{24}$$

At the shock, the solution satisfies

$$Y = 0 \quad \text{and} \quad \theta = \frac{B_T}{B^+}J^+ = \frac{B_T}{B^-}J^- \qquad \text{at} \quad \xi = 0, \tag{25}$$

corresponding to a chemically frozen shock wave. As shown in,[12] the equations $\theta = (B_T/B^+)J^+ = (B_T/B^-)J^-$ follow from linearization of the Rankine-Hugoniot jump conditions, with the factors B_T/B^+ and B_T/B^- evaluated from the expressions

$$B_T = \frac{1}{F_T}\frac{\partial F_T}{\partial \sigma} \quad \text{and} \quad B^{\pm} = \frac{1}{F_p}\frac{\partial F_p}{\partial \sigma} \mp \frac{\gamma M_o^2}{\sqrt{M_o^2-1}}\frac{\partial F_\nu}{\partial \sigma} \tag{26}$$

involving the functions $T/T' = F_T(M', \sigma)$, $p/p' = F_p(M', \sigma)$, and $\nu = F_\nu(M', \sigma)$ for the jumps in temperature and pressure and for the clockwise flow deflection across the shock as a function of the incident angle σ and upstream Mach number M'.

IV. Critical ignition conditions

IV.A. The eigenvalue problem

Integration of (19)–(21) with the boundary condition stated in (24) and (25) determines D as an eigenvalue. The solution can be simplified by eliminating the pressure gradient in (20) by linear combinations with (25) to give

$$\frac{\partial\theta}{\partial\xi} = \left[1 - \frac{(\gamma-1)(\tan^2\mu_o+1)}{(\tan\mu_o/\tan\phi_o)^2-1}\right] D(Y+\bar{\lambda}Y^{1/2})e^{-\eta^2-\xi}e^{\theta}. \tag{27}$$

A chemistry-free linear combination of the equation for J^- with this last equation provides

$$\theta + \frac{B_T}{B^-}\kappa J^- = \theta_s(1+\kappa) \tag{28}$$

upon integration with the boundary condition at $\xi = 0$, where $\theta = \theta_s(\eta)$. The parameter

$$\kappa = \frac{B^-}{\gamma B_T}\frac{\tan\mu_o/\tan\phi_o - 1}{\tan^2\mu_o+1}\left[1 - \frac{(\gamma-1)(\tan^2\mu_o+1)}{(\tan\mu_o/\tan\phi_o)^2-1}\right] \tag{29}$$

measures the competition between the cooling rate associated with the flow expansion induced by the chemical reaction and the direct heat release of the chemical reaction. Its value can be computed in terms of the upstream values of the incident angle σ_o and incident Mach number M_o' at $z = z_o$, giving values $\kappa > -1$ of order unity (see Fig. 3 in ref.[12]). Negative values of κ correspond to temperature perturbations that decrease along the stretched streamline coordinate ξ.

The problem reduces to the integration of (19) and (27) subject to the boundary conditions $\theta - \theta_s = Y = 0$ at $\xi = 0$ and $\theta = (1+\kappa)\theta_s$ at $\xi = \infty$, the latter obtained by evaluating (28). To reduce the parametric dependence, it is convenient to introduce the rescaled H_2O_2 concentration

$$\varphi = \left(\frac{\gamma B_T}{B^-}\frac{\tan^2\mu_o+1}{\tan\mu_o/\tan\phi_o-1}\right)^{2/3} Y \tag{30}$$

to yield

$$\frac{\partial\varphi}{\partial\xi} = \Delta\varphi^{1/2}e^{-\eta^2-\xi}e^{\theta} \tag{31}$$

$$\frac{\partial\theta}{\partial\xi} = \kappa\Delta(\varphi+\lambda\varphi^{1/2})e^{-\eta^2-\xi}e^{\theta}, \tag{32}$$

subject to

$$\varphi = \theta - \theta_s = 0 \quad \text{at} \quad \xi = 0 \qquad \text{and} \qquad \theta = (1+\kappa)\theta_s \quad \text{at} \quad \xi = \infty, \tag{33}$$

where

$$\Delta = \left(\frac{\gamma B_T}{B^-}\frac{\tan^2\mu_o+1}{\tan\mu_o/\tan\phi_o-1}\right)^{1/3} D \quad \text{and} \quad \lambda = \left(\frac{\gamma B_T}{B^-}\frac{\tan^2\mu_o+1}{\tan\mu_o/\tan\phi_o-1}\right)^{1/3}\bar{\lambda}. \tag{34}$$

IV.B. The critical Damköhler number

Dividing (32) by (31) and integrating yields

$$\theta - \theta_s = \kappa\left(\frac{2}{3}\varphi^{3/2} + \lambda\varphi\right) \tag{35}$$

after using the boundary condition at the shock. This last equation relates the temperature perturbations and the rescaled H_2O_2 concentration everywhere and can be used in particular to yield

$$\theta_s(\eta) = \frac{2}{3}\varphi_\infty(\eta)^{3/2} + \lambda\varphi_\infty(\eta) \tag{36}$$

as an implicit equation for the far-field concentration φ_∞ corresponding to a given streamline in terms and the associated post-shock temperature θ_s. Using (35) in (31) and integrating gives

$$\int_0^{\varphi}\frac{\mathrm{d}\varphi}{\varphi^{1/2}\exp\left[\kappa\left(\frac{2}{3}\varphi^{3/2}+\lambda\varphi\right)\right]} = \Delta e^{-\eta^2}\exp\left(\frac{2}{3}\varphi_\infty^{3/2} + \lambda\varphi_\infty\right)(1-e^{-\xi}), \tag{37}$$

for $\varphi(\xi,\eta)$, which can be evaluated at $\xi=\infty$ to give

$$\int_0^{\varphi_\infty} \frac{\mathrm{d}\varphi}{\varphi^{1/2}\exp\left[\kappa\left(\frac{2}{3}\varphi^{3/2}+\lambda\varphi\right)\right]} = \Delta e^{-\eta^2}\exp\left(\frac{2}{3}\varphi_\infty^{3/2}+\lambda\varphi_\infty\right), \tag{38}$$

which determines explicitly the far-field concentration $\varphi_\infty(\eta)$ for given values of Δ, κ, and λ.

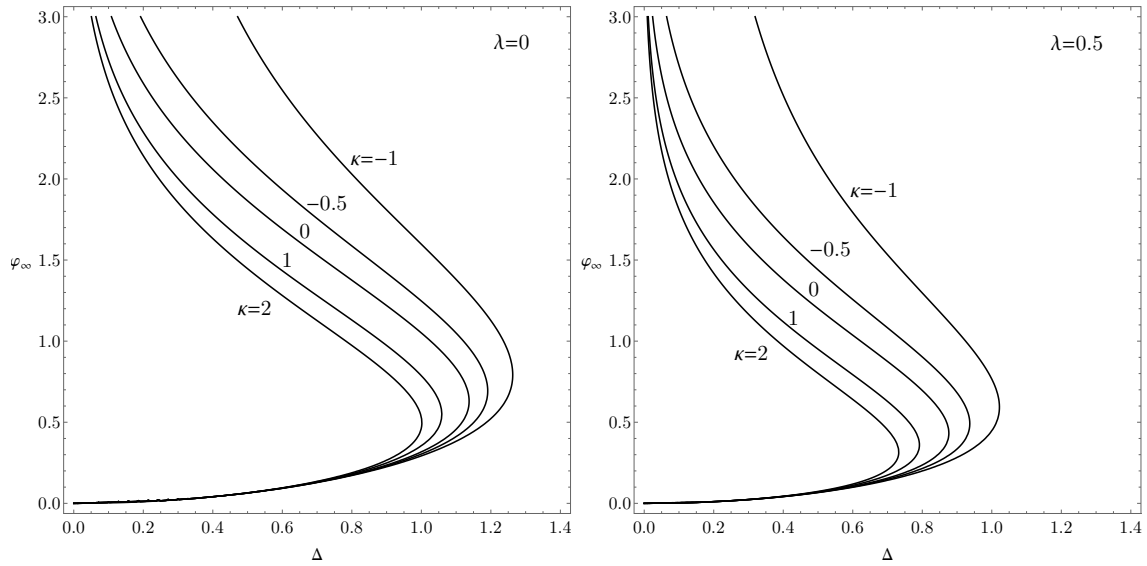

Figure 3. The normalized peak H_2O_2 concentration $\varphi_\infty(0)$ as a function of the ignition Damköhler number Δ obtained by evaluation of (39).

The explosion diagram can be obtained by using the above equation to evaluate the ignition Damköhler number Δ as a function of the peak concentration $\varphi_\infty(0)$ according to

$$\Delta = \frac{1}{\exp\left[\frac{2}{3}\varphi_\infty^{3/2}(0)+\lambda\varphi_\infty(0)\right]}\int_0^{\varphi_\infty(0)} \frac{\mathrm{d}\varphi}{\varphi^{1/2}\exp\left[\kappa\left(\frac{2}{3}\varphi^{3/2}+\lambda\varphi\right)\right]}, \tag{39}$$

giving the results shown in Fig. 3 for $\lambda=0$ and $\lambda=0.5$ and different values of κ. As can be seen, the curves display a turning point at a value $\Delta=\Delta_c(\kappa,\lambda)$. This limiting value of Δ identifies the critical conditions for existence of a weakly reactive solution, in that two solutions are found for $\Delta<\Delta_c$ while no solution exists for $\Delta>\Delta_c$. Correspondingly, the values $\Delta=\Delta_c(\kappa,\lambda)$ at the turning points in Fig. 3 (which may be compared with Fig. 4 in Ref.[12]) together with the definitions given in (22), (23), (29) and (34) for κ, λ, and Δ provide the information needed to evaluate the critical conditions for low-temperature ignition in hydrogen-air mixing layers.

V. Discussion of Results

The results of the present analysis, such as those shown in Fig. 3, determine the critical conditions needed for an oblique shock to produce ignition in the supersonic mixing layer, defined by $\Delta=\Delta_c$. Since ignition below the crossover temperature involves a thermal runaway process like that analyzed previously for a simpler one-step Arrhenius description of the chemistry,[12] the parametric dependences of these ignition conditions are basically the same as those found in that previous work. In particular, the relevant heating-rate parameter κ is exactly the same, and its influence on the predictions has been discussed before.[12] The difference for the present hydrogen-chemistry problem involves the definition of the Damköhler number and the necessity of including a differential equation for the variation of the concentration of H_2O_2. The latter introduces the additional parameter λ, which measures the additional heat release associated with the formation of H_2O_2. Comparison of the two graphs in Fig. 3, for example, indicates that, at a fixed Damköhler number based on the heat release associated with the formation of H_2O, an increase in the heat

release associated with the formation of H_2O_2 decreases the critical value of the Damköhler number required for ignition, as would be expected.

Sufficiently strong shock waves increase the temperature of the hydrogen-air mixture to levels high enough to produce ignition. In particular, once the post-shock mixture temperature reaches or exceeds the crossover temperature, ignition may be expected to occur. Ignition may, however, also be generated by weaker shocks that do not raise the gas temperature to crossover, if the critical value $\Delta = \Delta_c$ is exceeded. This would occur at sufficiently large values of the Damköhler number D in (22), of order unity. This ratio of cooling time to chemical time is affected by flow-configuration parameters, such as the thickness δ of the mixing layer and the order-unity nondimensional measure Λ of the rate of acoustic cooling, increasing in proportion to the ratio δ/Λ, which combines with U_o to determine the relevant cooling time. It thus becomes clear that at sufficiently high pressures (so that the chemical time is short enough) or for sufficiently thick mixing layers, the present analysis can be applied to determine a critical shock angle and shock strength that would lead to ignition at post-shock temperatures below crossover.

A representative experiment[21] may be considered for illustrating the nature of these prediction. In that experiment, at a pressure of about 40 kPa, a supersonic air stream at a temperature of around 700 K and a Mach number of 2 mixes with a cooler hydrogen stream flowing at a Mach number of 1.7. Although the experimental ignition techniques did not rely upon a shock wave, it is of interest to investigate how strong a shock would be required to produce ignition. This is done here for hydrogen-stream Mach numbers between 1.4 and 2, for a higher air Mach number of 3, which may be more representative of a hypersonic-flight application, with an estimated mixing-layer thickness of $\delta = 0.05$ m, at three different air-stream temperatures. To make certain that the peak temperature and ignition occur in the interior of the mixing layer rather than at the air boundary, both streams are assigned the same initial temperature. The results, summarized in Fig. 4, indicate that, throughout this range of conditions, oblique-shock-induced ignition occurs when the temperature behind the shock, at angle σ_o, reaches the crossover temperature; mixing-layer thicknesses on the order of 1 m, or pressures in excess of 10 atm would be needed to achieve ignition at lower post-shock temperatures.

Figure 4 shows that, as expected, the oblique-shock angle needed for ignition decreases with increasing approach-stream temperatures. It also decreases with increasing hydrogen-stream Mach numbers because of the associated increased kinetic energy producing higher peak temperatures in the interior of the mixing layer through increased dissipation. Pre-shock properties at the ignition kernel, M_o', T_o', p_o', and Y_o, have been obtained by computing the mixing-layer profiles for the above-mentioned feed-stream conditions (see ref.[22] for details). Contours of constant values of the air-stream shock angle σ_∞ and shock strength p_∞/p' are also shown in the figure, based on the Moeckel approximation,[14] suggesting that relatively weak incident shocks would be sufficient under these conditions. It may be noted[12] that the basis of the present analysis for ignition occurring at post-shock temperatures below crossover, requiring a positive value of Λ of order unity, is valid only in the region between the neutral-transmission curve and the weak-shock limit in this figure, since Λ approaches zero at the weak-shock limit and becomes negative, corresponding to acoustic compression rather than expansion waves, above the neutral-transmission curve. The range of applicability becomes much larger at higher Mach numbers.

VI. Conclusions

By use of a justified two-step reduced-chemistry description for hydrogen-air systems, an analysis has been developed which provides the critical conditions for mixing-layer ignition by shock-wave impingement under conditions such that the temperature in the ignition kernel prior to ignition remains below the crossover temperature. The analysis, based on investigations of small departures from the chemically frozen post-shock state, with the critical ignition conditions identified by the turning point in the bifurcation curve representing the peak reactive perturbation as a function of the ignition Damköhler number (measuring the ratio of the residence time to the relevant chemical time evaluated at the peak temperature of the unperturbed base flow), becomes useful at sufficiently high pressures for sufficiently large mixing-layer thicknesses and Mach numbers. Otherwise a simpler analysis, equating the post-shock ignition-kernel temperature to the crossover temperature, would apply, corresponding to a branched-chain rather than thermal explosion. These two different chemical-kinetic processes thus characterize hydrogen-air diffusion-flame ignition by shock-wave impingement on supersonic mixing layers under different conditions.

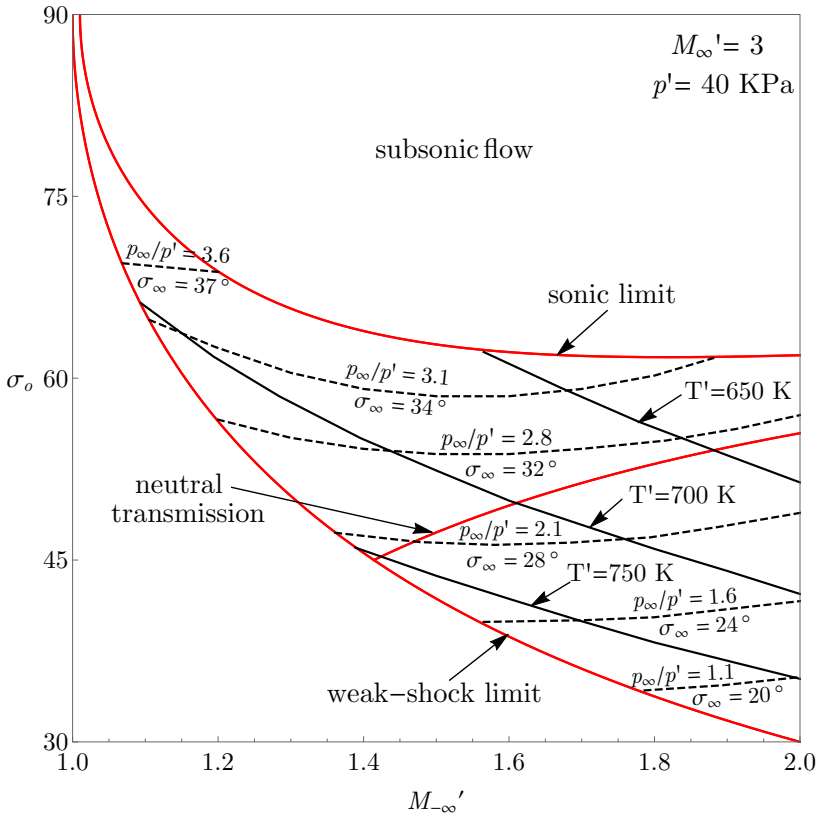

Figure 4. A representative calculated variation of the shock angle at the ignition kernel with the hydrogen-stream Mach number for producing post-shock crossover temperatures at three different approach-flow temperatures, with corresponding shock angle and shock strength in the air stream identified by dashed curves.

Acknowledgments

This work was supported by the US AFOSR Grant # FA9550-12-1-0138 and by the Spanish MCINN through the Program CONSOLIDER-Ingenio2010 (Project No. CSD2010-00011).

References

[1]Ferri, A., "Mixing-Controlled Supersonic Combustion," *Annual Review of Fluid Mechanics*, Vol. 5, 1973, pp. 301–338. doi:10.1146/annurev.fl.05.010173.001505

[2]Andreopoulos, Y., Agui, J. H., and Briassulis, G., "Shock Wave-Turbulence Interactions," *Annual Review of Fluid Mechanics*, Vol. 32, 2000, pp. 309–345. doi:10.1146/annurev.fluid.32.1.309

[3]Dolling, D. S., "Fifty Years of Shock-Wave/Boundary-Layer Interaction Research: What Next?," *AIAA Journal*, Vol. 39, No. 8, 2001, pp. 1517–1531. doi: 10.2514/2.1476

[4]Waidmann, W., Alff, F., Brummund, U., Böhm, M., Clauss, W., and Oschwald M., "Experimental Investigation of the Combustion Process in a Supersonic Combustion Ramjet (SCRAMJET)," In: DLR Jahrestagung, pp. 629-638, Erlangen, 1994 doi:

[5]Laurence, S. J., Karl, S., Schramm, J., Martínez, J. and Hannemann, K., "Transient Fluid-Combustion Phenomena in a Model Scramjet," *Journal of Fluid Mechanics*, Vol. 722, 2013, pp. 85–120. doi: 10.1017/jfm.2013.56

[6]Gutmark, E. J., Schadow, K. C., and Yu, K. H., "Mixing Enhancement in Supersonic Free Shear Flows," *Annual Review of Fluid Mechanics*, Vol. 27, 1995, pp. 375–417. doi: 10.1146/annurev.fl.27.010195.002111

[7]Menon, S., "Shock-Wave-Induced Mixing Enhancement in Scramjet Combustors," *AIAA Paper* 89-0104, 1989. doi: 10.2514/6.1989-104

[8]Lu, P. J. and Wu, K. C., "On the Shock Enhancement of Confined Supersonic Mixing Flows," *Physics of Fluids A*, Vol. 3, 1991, pp. 3046–3062. doi: 10.1063/1.857849

[9]Marble, F. E., "Gasdynamic Enhancement of Nonpremixed Combustion," *Proceedings of the Combustion Institute*, Vol. 25, 1994, pp. 1–12. doi: 10.1016/S0082-0784(06)80621-1

[10]Brummund, U. and Nuding, J. R.,"Interaction of a Compressible Shear Layer with Shock Waves - An Experimental Study," *AIAA Paper* 97–0392, 1997. doi: 10.2514/6.1997-392

[11]Kevlahan, N. K-R.,"The Propagation of Weak Shocks in Non-uniform Flows," *Journal of Fluid Mechanics*, Vol. 327, 1991, pp. 161–197. doi: 10.1017/S0022112096008506

[12]Huete, C., Sánchez, A. L., Williams, F. A., and Urzay, J., "Diffusion-Flame Ignition by Shock-Wave Impingement on a Supersonic Mixing Layer," *Journal of Fluid Mechanics*, Vol. 784, 2015, pp. 74–108. doi: 10.1017/jfm.2015.585

[13]Sánchez, A. L. and Williams, F. A., "Recent Advances in Understanding of Flammability Characteristics of Hydrogen," *Progress in Energy and Combustion Science*, Vol. 41, 2014, pp.1–55. doi: 10.1016/j.pecs.2013.10.002

[14]Moeckel, W. E., 'Interaction of Oblique Shock Waves with Regions of Variable Pressure, Entropy, and Energy," *NACA Techical Note* 2725, 1952, pp. 35. doi:

[15]Liñán, A. and Crespo A.,"An Asymptotic Analysis of Unsteady Diffusion Flames for Large Activation Energies," *Combustion Science and Technololgy*, Vol. 14, 1976, pp. 95–117. doi: 10.1080/00102207608946750

[16]Jackson, T. L. and Hussaini M. Y.,"An Asymptotic Analysis of Supersonic Reacting Mixing Layers," *Combustion Science and Technololgy*, Vol. 57, 1988, pp. 129–140. doi: 10.1080/00102208808923948

[17]Boivin, P., Sánchez, A. L. and Williams, F. A., "Explicit Analytic Prediction for Hydrogen-Oxygen Ignition Times at Temperatures Below Crossover," *Combustion and Flame*, Vol. 159, 2012, pp. 748-752. doi: 10.1016/j.combustflame.2011.08.019

[18]Fernández-Tarrazo, E., Sánchez, A. L., and Williams, F. A., "Hydrogen-Air Mixing-Layer Ignition at Temperatures Below Crossover," *Combustion and Flame*, Vol. 160, 2013, pp. 1981–1989. doi: 10.1016/j.combustflame.2013.04.027

[19]Sánchez, A. L. and Williams, F. A., "The Chemistry Involved in the Third Explosion Limit of H_2-O_2 Mixtures," *Combustion and Flame*, Vol. 161, 2014, pp. 111–117. doi: 10.1016/j.combustflame.2013.07.013

[20]Hayes, W. D. and Probstein, R. F. *Hypersonic Inviscid Flow*, Second ed., Dover, Mineola, NY, pp. 480–484, 2004.

[21]Rockwell, R. D., Goyne C. P., Rice B. E., Kouchi, T., and McDaniel, J.C., "Collaborative Experimental and Computational Study of a Dual-Mode Scramjet Combustor," *Journal of Propulsion and Power*, Vol. 30, No. 3, 2014, pp. 530-538. doi: 10.2514/1.B35021

[22]Huete, C., Urzay, J., Sánchez, A. L., and Williams, F. A., "Weak-Shock Interactions with Transonic Laminar Mixing Layers of Fuels for High-Speed Propulsion," *AIAA Journal*, Vol. 54, 2016, pp. pending doi: 10.2514/1.J054419